Hypersonic Boundary Layer/Shockwave Interaction Problems

Haile Lindsay[1] and Frederick Ferguson[2]
Center for Aerospace Research
North Carolina A&T State University
Greensboro, North Carolina 27411

Abstract

The hypersonic shockwave boundary layer-interaction problem was defined with the use of the full Navier-Stokes (NS) equations and a FORTRAN code was developed to provide numerical solutions to this problem. Further, this problem was studied under two specified sets of boundary conditions: adiabatic wall and constant wall conditions. The MacCormack Predictor-Corrector technique was used in developing this NS code. To validate the numerical code, the flat plate problem was solved, and the results compared to that published in established journals. In solving these problems, engineering tools such as, FORTRAN, TECPLOT, and EXCEL, were used to generate plots of the primitive variables, such as, the velocity components, u and v, and the temperature T. Selected plots were reproduced from various references in validating the work done for the flat plate and hypersonic shockwave boundary layer interaction problems. All preliminary results indicated that the code was validated and the results obtained were in accordance of the physical behavior of the flow fields. Now that an aerospace engineering tool was developed, it is recommended that future designers seek to further its development by making the code user-friendly and that they further test accuracy of the code by solving other 2D fluid dynamic problems.

Nomenclature

ρ	density
u	velocity in the x-direction
v	velocity in the y-direction
e	energy
T	temperature
V	total velocity
q_x	heat transfer in the x-direction
q_y	heat transfer in the y-direction
p	pressure
μ	dynamic (absolute) viscosity
ν	kinematic viscosity
τ_{xx}	normal shear stress in x direction
τ_{yy}	shear stress in the y direction
τ_{yx}	shear stress perpendicular to y plane
τ_{xy}	same as τ_{yx}
k	thermal conductivity
R_{gas}	universal gas constant

[1] PhD Student, Department of Mechanical Engineering, Greensboro, NC 27411
[2] Director for Center for Aerospace Research, Associate Professor, Department of Mechanical Engineering Greensboro, NC 27411

ρ_∞	density at freestream conditions
M_∞	Mach Number at freestream conditions
P_∞	pressure at freestream conditions
a_∞	speed of sound at freestream conditions
u_∞	x-component of the velocity at freestream conditions
v_∞	y-component of the velocity at freestream conditions
T_∞	temperature at freestream conditions
Pr_∞	Prandtl number at freestream conditions
L	length of the plate
γ	ratio of c_p over c_v
IMAX	the number of points in the x-direction
IMIN	the least numbered point in the x-direction
JMAX	the number of points in the y-direction
JMIN	the least numbered point in the y-direction
Δx	incremental change in the x-direction
Δy	incremental change in the y-direction
Δt	incremental change in time
a	speed of sound
c_p	specific heat using constant pressure
c_v	specific heat using constant volume
θ	deflection angle
β	wave angle
i	index used to move in the x-direction
j	index used to move in the y-direction
y_{bar}	normalized y
C_f	skin friction coefficient
τ_w	shear stress along the wall
$\nu'_{i,j}$	maximum value of kinematic viscosity that will be applied in solving the time step
Pr	Prandtl number

1.0 Introduction

The world of aeronautics experienced a great loss in February 2003 when the Space Shuttle Columbia blew up. The seven astronauts on board were killed while returning to the Earth's atmosphere. Safety issues were a key factor in this occurrence. One of the ways to correct problems of safety in space shuttles is to examine how primitive variables such as velocity components u and v, temperature, and density behave.

In general, the conservation laws, the conservation of mass, the conservation of momentum, and the conservation of energy dictate the behavior of the primitive variables. These laws, when combined, are known as the Navier-Stokes (N-S) equations. These equations are further discussed in the next section and they can be solved either

analytically or numerically. The numerical solution of the N-S equations for laminar flow over a flat plate is discussed in the next section. However, there are various numerical techniques that can be utilized to solve the N-S equations. Two of these numerical techniques are the Lax-Wendroff Technique and the Crank-Nicholson Technique.

The Lax-Wendroff Technique is a finite difference scheme that was derived by Lax and Wendroff in 1960, [1]. It is an explicit scheme suitable for time or space marching solutions. In other words, the solution process allows for the advancement of the primitive variables in either time or space.

Crank and Nicholson derived the Crank-Nicholson Technique in 1947. It is a second order accurate scheme that uses trapezoidal differencing. This particular technique was first used to solve the partial differential heat conduction equation. The researchers studied the development of numerical techniques. However, at the University of Maryland at College Park, Adam Grumet and Charles Bollaro [2, 3] conducted research on hypersonic boundary layer-shockwave interaction utilizing the MacCormack Technique with certain freestream conditions. The MacCormack Technique is the technique utilized in this paper because of its simplicity and accuracy.

A real life example of understanding the importance of hypersonic boundary layer-shockwave interaction would be in the designing of a generic hypersonic vehicle powered by a SCRAMjet engine as illustrated in Figure 1. From the study conducted herein, one can understand how velocity and heat transfer are related. Designers can also predict how the SCRAMjet performance might be affected as the vehicle travels in space.

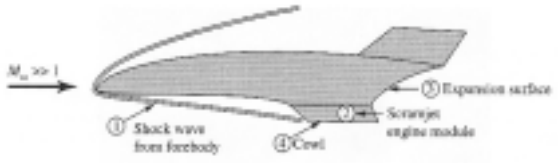

Figure 1. A Hypersonic Vehicle

2.0 Governing Equations

Solving any problem involving fluid flows involves mechanical engineering relations of the various flow field properties such as mass flux, and so forth, at any given point in the flow field. Designers find the most applicable laws to derive these engineering relations to be the conservation laws. When applied to fully viscous flow, the equations are termed the Navier-Stokes equations. Solution of the N-S equations fully accounts for the effects of viscosity in the shear and normal viscous stress terms that show up in both the conservation of momentum and conservation of energy equations.

The two-dimensional N-S equations from the laws of mass, momentum (x and y components), and energy in its nonconservative differential form for a perfect or ideal gas is as follows:

$$\frac{\partial \rho}{\partial t}+\frac{\partial(\rho u)}{\partial x}+\frac{\partial(\rho v)}{\partial y}=0 \qquad (1a)$$

$$\rho\frac{Du}{Dt}=-\frac{\partial p}{\partial x}+\frac{\partial \tau_{xx}}{\partial x}+\frac{\partial \tau_{yx}}{\partial y} \qquad (1b)$$

$$\rho\frac{Dv}{Dt}=-\frac{\partial p}{\partial y}+\frac{\partial \tau_{xy}}{\partial x}+\frac{\partial \tau_{yy}}{\partial y} \qquad (1c)$$

$$\rho\frac{D\left(e+\frac{V^2}{2}\right)}{Dt}=\rho\dot{q}+\frac{\partial q_x}{\partial x}+\frac{\partial q_y}{\partial y}-\frac{\partial(up)}{\partial x}-\frac{\partial(vp)}{\partial y}+\frac{\partial(u\tau_{xx})}{\partial x}+\frac{\partial(u\tau_{yx})}{\partial y}+\frac{\partial(v\tau_{xy})}{\partial x}+\frac{\partial(v\tau_{yy})}{\partial y} \qquad (1d)$$

with the viscous stresses involved as follows:

$$\tau_{xx} = \frac{2}{3}\mu\left(2\frac{\partial u}{\partial x} - \frac{\partial v}{\partial y}\right) \quad (2a) \qquad \tau_{yy} = \frac{2}{3}\mu\left(2\frac{\partial v}{\partial y} - \frac{\partial u}{\partial x}\right) \quad (2b) \qquad \tau_{xy} = \tau_{yx} = \frac{2}{3}\mu\left(\frac{\partial u}{\partial y} + \frac{\partial v}{\partial x}\right) \quad (2c)$$

along with the heat transfer terms that are involved: [6]

$$q_x = -k\frac{\partial T}{\partial x} \quad (3a) \qquad q_y = -k\frac{\partial T}{\partial y} \quad (3b)$$

The N-S equations can be expressed as a single vector equation of the first order using the vectors U, E, and F. They can be stated in the following form:

$$\frac{\partial U}{\partial t} + \frac{\partial (E_{inv} + E_{vis})}{\partial x} + \frac{\partial (F_{inv} + F_{vis})}{\partial y} = 0 \quad (4)$$

where $\partial U/\partial t$ is partial derivative of the solution vector with respect to time, E_{inv} is the inviscid portion of the flux vector in the x direction, E_{vis} the viscous portion of the flux vector in the x direction, F_{inv} is the inviscid portion of the flux vector in the y direction, and F_{vis} is the viscous portion of the flux vector in the y direction. The arrangement of how these equations were placed in vector form can be found within reference 13. According to Grumet [2], a major reason for utilizing the vector form of the N-S equations is because when a flow goes across a shock wave, the flux variables are continuous, while the primitive variables are discontinuous. Another important reason why it is better to utilize the vector form instead of the non-vector form because the vector form deals with the flux variables like ρv, ρuv, etc. while, on the other hand, the non-vector form deals only in the primitive variables, ρ, v, and u. The non-vector form of equations is in theory valid for flow across a shock. However, when it is applied using a numerical technique or scheme, the results that are produced are not correct and yet when the vector form of the equations are used going across a shock, the results are solid.

3.0 MacCormack Technique

From an analytical standpoint, the N-S equations cannot be solved; therefore, various numerical methods must be implemented to provide a solution for designers of future spacecrafts.

The particular technique of interest to this paper is the MacCormack Technique. This technique, which came into existence in 1969, is second order accurate in both space and time. It is an explicit, time dependent scheme that is capable of solving combined hyperbolic-elliptic flow fields, such as those encountered in supersonic and subsonic flow flight regimes.

To effectively employ this numerical technique to solve the laminar flow over a flat plate, a numerical two-dimensional domain must be described and a set of rectangular grids be constructed (see Figure 2). In the process, care should be taken to ensure that the surface of the plate, the freestream, and the other boundary conditions are adequately described.

Each of the grid points receives from the beginning primitive flow variables, which in turn can be transformed into flux variables. The flow values of each of the flow variables then serve as the initial conditions for this MacCormack Technique that marches in time. In this paper, in order for the flow field to converge properly to a steady state solution, the use of uniform freestream conditions will be applied.

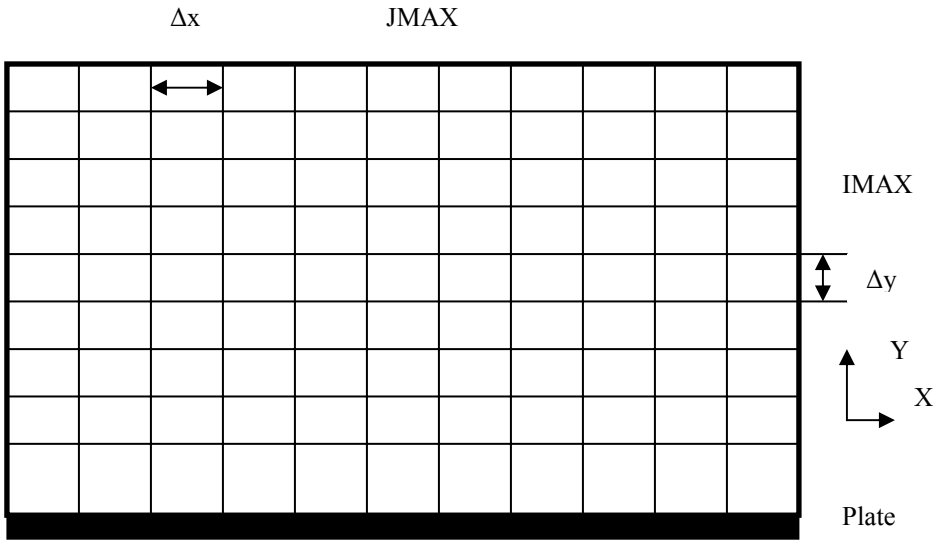

Figure 2. Rectangular Grid Corresponding to Flow over a Flat Plate

Utilizing the initial conditions, the flow field is recalculated at each particular grid point in time steps, Δt, using the Taylor Series expansion:

$$U(t+\Delta t) = U(t) + \left(\frac{\partial U}{\partial t}\right)_{av} * \Delta t \tag{5}$$

where U(t + Δt) is the solution vector at a time t + Δt, U(t) is the original solution at time t, $\partial U/\partial t_{av}$ is the average partial derivative of the solution vector U with respect to time, and Δt is the change that is calculated through a stability study.

3.1 Calculating $\partial U/\partial t_{av}$

In calculating $\partial U/\partial t_{av}$, the following equation is used:

$$\left(\frac{\partial U}{\partial t}\right)_{av} = \frac{1}{2}\left(\left(\frac{\partial U}{\partial t}\right)_{b} + \left(\frac{\partial U}{\partial t}\right)_{f}\right) \tag{6}$$

where the average is taken between the partial derivatives of the solution vector with respect to time from both the predictor step ($\partial U/\partial t_f$) and the corrector step ($\partial U/\partial t_b$). This equation is used to gain the steady state solution of the flowfield by going on in time, until all the flow variables converge with respect to time.

3.2 Calculating $\partial U/\partial t_b$ and $\partial U/\partial t_f$

MacCormack's Technique solves the first order Taylor series given in Equation 5 by creatively predicting and then correcting the time derivative in a manner that achieves second order accuracy. The MacCormack Technique, broken down in its predictor and corrector nature, is described in the following sections. In both the predictor and corrector steps, the following equation is used to calculate the partial derivative of U with respect to t in utilizing both backward and forward differencing:

$$\left(\frac{\partial U}{\partial t}\right)_{b,f} = -\left[\frac{\partial E}{\partial x} + \frac{\partial F}{\partial y}\right] \tag{7}$$

In the predictor step, the use of forward differencing comes into play. Below is the basic forward differencing formula that will be used in calculating the derivatives of the E and F vectors [7]:

$$\frac{df}{dx}(x_i) = \frac{f_{i+1} - f_i}{\Delta x} \tag{8}$$

The vectors E and F were evaluated using forward differencing as follows:

$$\frac{\partial E}{\partial x} = \frac{E_{i+1,j}{}^t - E_{i,j}{}^t}{\Delta x} \tag{9}$$

and:

$$\frac{\partial F}{\partial y} = \frac{F_{i,j+1}{}^t - F_{i,j}{}^t}{\Delta y} \tag{10}$$

In this step, whenever the variable $\partial u/\partial x$ is being calculated within the vectors, E and F, (see equation 2(a)), the backward differencing was utilized as suggested by Abbott [8]. The backward differencing formula in first order is as follows [8]:

$$\frac{db}{dx}(x_i) = \frac{b_i - b_{i-1}}{\Delta x} \tag{11}$$

Whenever the variable $\partial u/\partial y$ is being calculated within the vectors, E and F, (see equation 2(c)), the central differencing was utilized [8] as follows:

$$\frac{dc}{dx}(x_i) = \frac{c_{i+1} - c_{i-1}}{2\Delta x} \tag{12}$$

In the corrector step, the use of backward differencing comes into play. Equation 11 plays the major role in solving for the vectors E and F. These variables were evaluated using backward differencing as follows:

$$\frac{\partial E}{\partial x} = \frac{E_{i,j}{}^t - E_{i-1,j}{}^t}{\Delta x} \tag{13}$$

and:

$$\frac{\partial F}{\partial y} = \frac{F_{i,j}{}^t - F_{i,j-1}{}^t}{\Delta y} \tag{14}$$

As described earlier, in this step, whenever the variable $\partial u/\partial x$ is being calculated within equation 13, the central differencing procedure is applied. Similarly, in this step, whenever the variable $\partial u/\partial y$ is being calculated within equation 14, the forward differencing, equation 8 is applied.

3.3 Calculating Δt

The MacCormack Technique is an explicit, numerical technique and as such, it is subjected to stability criteria. In this study, a version of the CFL or Courant-Frederichs-Lewy Condition is used to calculate the size of the time step for each iterative cycle. In getting the best value for the time step, a fudge factor K, termed the Courant number

is applied. This factor is generally in the range of 0.5 and 0.8 and serves to keep the solution stable. In this paper, a value of 0.7 was used. The equations used to compute the time step are as follows:

$$\left(\Delta t_{CFL}\right)_{i,j} = \left[\frac{\left|u_{i,j}\right|}{\Delta x} + \frac{\left|v_{i,j}\right|}{\Delta y} + a_{i,j}\sqrt{\frac{1}{\Delta x^2} + \frac{1}{\Delta y^2}} + 2\nu'_{i,j}\left(\frac{1}{\Delta x^2} + \frac{1}{\Delta y^2}\right)\right]^{-1} \tag{15}$$

where:

$$\nu'_{i,j} = \max\left[\frac{\frac{4}{3}\mu_{i,j}, \left(\frac{\gamma\mu_{i,j}}{\Pr}\right)}{\rho_{i,j}}\right] \tag{16}$$

and:

$$a_{i,j} = \sqrt{\gamma RT} \tag{17}$$

It is of interest to note that the Δt is computed at each grid point. Once the time study is completed, the smallest time step is chosen in accordance with:

$$\Delta t = \min\left[K\left(\Delta t_{CFL}\right)_{i,j}\right] \tag{18}$$

The implementation of MacCormack Technique within this study can be found in my thesis.

4.0 Problems Solved

In this study, two problems were solved: the normal flat plate problem that was prescribed by Anderson's *Computational Fluid Dynamics* and the hypersonic boundary layer/shockwave interaction problem. In this particular section, there are two tables: one with the variables for both cases and the other containing the boundary conditions that were applied to both cases.

Table I. Freestream Conditions for both cases

Parameters	***Normal Flat Plate***	***Hypersonic Boundary Layer Shockwave Interaction***	
M_∞	4.0	5.0	
a_∞	340.28	340.28	m/s
P_∞	101325.0	101325.0	Pa
μ_∞	1.7894e-05	1.7894e-05	kg/(m*s)
u_∞	1361.12	1361.12	m/s
Γ	1.4	1.4	
Pr_∞	0.71	0.71	
R_{gas}	287.0	287.0	J/(kg*K)
T_∞	288.16	288.16	°K
v_∞	0.0	0.0	m/s
C_v	2.5	2.5*Rgas	
C_p	3.5	3.5*Rgas	
Θ	0.0	20	Degrees
ß	0.0	30	Degrees

Table II. Boundary Conditions for both cases

Conditions	***Normal Flat Plate Problem***	***Hypersonic Boundary Layer Shockwave Interaction***
Leading Edge	$\rho_{1,1} = 1.0$ $u_{1,1} = 0.0$ $v_{1,1} = 0.0$ $T_{1.1} = \frac{R_{gas} T_\infty}{u_\infty{}^2}$	Same as Flat Plate
Inflow Conditions *(i = 1, j = 1, JMAX+1)*	$\rho_{1,j} = 1.0$ $u_{1,j} = 1.0$ $v_{1,j} = 0.0$ $T_{1.j} = \frac{R_{gas} T_\infty}{u_\infty{}^2}$	Same as Flat Plate
Surface Constant Temperature Conditions *(i = 1, IMAX+1, j = 1)*	$\rho_{i,1} = 2.0 * \rho_{i,2} - \rho_{i,3}$ $u_{i,1} = 0.0$ $v_{i,1} = 0.0$ $T_{i.1} = \frac{R_{gas} T_{wall}}{u_\infty{}^2}$	Same as Flat Plate
Surface Adiabatic Temperature Conditions *(i = 1, IMAX+1, j = 1)*	$\rho_{i,1} = 2.0 * \rho_{i,2} - \rho_{i,3}$ $u_{i,1} = 0.0$ $v_{i,1} = 0.0$ $T_{i.1} = T_{i,2}$	Same as Flat Plate
Upper Boundary Conditions *(i = 1, IMAX+1,* *j = JMAX)*	$\rho_{i,JMAX} = 1.0$ $u_{i,JMAX} = 1.0$ $v_{i,JMAX} = 0.0$ $T_{i.JMAX} = \frac{R_{gas} T_\infty}{u_\infty{}^2}$	Fixed conditions from equations 20 - 24
Outflow Conditions *(i = IMAX, j = 1, JMAX+1)*	$\rho_{IMAX,j} = 2.0 * \rho_{IMAX-1,j} - \rho_{IMAX-2,j}$ $u_{IMAX,j} = 2.0 * u_{IMAX-1,j} - u_{IMAX-2,j}$ $v_{IMAX,j} = 2.0 * v_{IMAX-1,j} - v_{IMAX-2,j}$ $T_{IMAX.j} = 2.0 * T_{IMAX-1,j} - T_{IMAX-2,j}$	Same as Flat Plate
Internal Points Initial Guess *(i = 2, IMAX-1,* *j = 2, JMAX-1)*	$\rho_{i,j} = 1.0$ $u_{i,j} = 1.0$ $v_{i,j} = 0.0$ $T_{i.j} = \frac{R_{gas} T_\infty}{u_\infty{}^2}$	Same as Flat Plate

5.0 Hypersonic Boundary Layer/Shockwave Interaction Problem

In this case, the study is focused on the interaction of a shockwave in a developing boundary layer. The freestream conditions are listed in Table I and its boundary conditions are listed in Table II. The objective of this study is the understanding of the boundary layer growth as it interacts with a 30-degree oblique shockwave in a Mach 5 flow field. The goal is to achieve a profile that resembles the predicted results as illustrated in Figure 3.

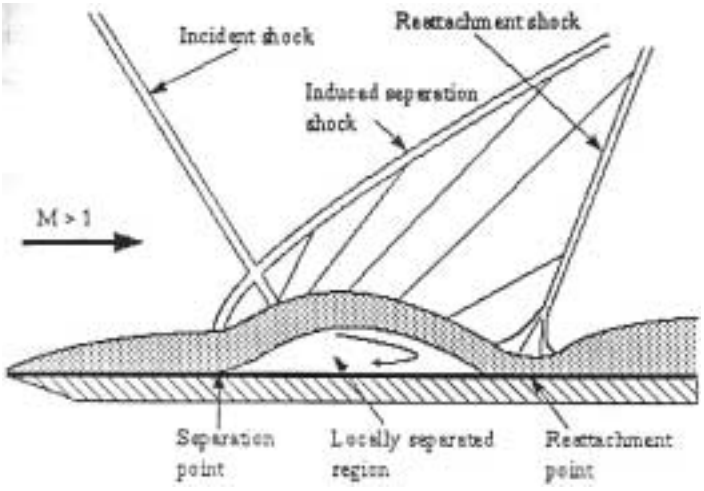

Figure 3. Hypersonic Boundary Layer/Shockwave Interaction

5.1 Calculating the Upper Boundary Conditions

In solving for the boundary conditions for Case II in the upper flow region, the θ-β-Mach number relationship has to come into effect. In this case, the Mach number is equal to 5.0 and beta is equal to 30 degrees. Using these parameters, theta can be found. From the beta-theta-Mach number relationship, the theta that is needed for this shock is 20 degrees. The plate length itself needs to be recalculated so that the shock will be as close to the center as possible and it is calculated as follows:

$$L = \frac{2.0 * D_h}{\tan\beta} \tag{19}$$

Equations 20 – 24 were used to calculate the values for the upper flow boundary condition that are shown in Table II. Note, that in solving for the u and v conditions, the values hinge on beta and theta only [12].

$$u = \frac{u_2}{u_1} = \frac{1}{1+\tan\theta\tan\beta} = \frac{1}{1+\tan 20\tan 30} = 0.826 \tag{20}$$

$$v = \frac{v}{v_1} = \frac{\tan\theta}{1+\tan\theta\tan\beta} = \frac{\tan 20}{1+\tan 20\tan 30} = 0.3008 \tag{21}$$

$$\rho = \frac{\rho_2}{\rho_1} = \frac{\gamma+1}{2} * \frac{M_\infty{}^2 \sin^2\beta}{1} + \frac{\gamma+1}{\gamma-1} = \frac{2.4}{2} * \frac{5^2 \sin^2 30}{1} + \frac{2.4}{0.4} = 3.33 \tag{22}$$

$$P = \frac{P_2}{P_1} = \frac{\frac{\gamma+1}{\gamma-1}\frac{\rho_2}{\rho_1} - 1}{\frac{\gamma+1}{\gamma-1} - \frac{\rho_2}{\rho_1}} = \frac{\frac{1.4+1}{1.4-1}(3.333) - 1}{\frac{1.4+1}{1.4-1} - 3.333} = 7.1 \tag{23}$$

$$T = \frac{T_2}{T_1} = \frac{P_2}{P_1} * \frac{\rho_1}{\rho_2} = 7.11 * \frac{1}{3.333} = 2.1351 \tag{24}$$

6.0 Results

6.1 Code Validation

In this study, grid independence was used to display the validity of the solver. The grid independence in this study involved the calculation of boundary layer thickness from what is known as "exact". The relationship δ/x is said to be 5.0 when the value of u/u_∞ is 0.99. In Table 3, notice that at the grid size 70 x 70, the value of this relationship is closer than any one of the other grid sizes in question and also has the smallest value of percent error. With 70 x 70 being the optimal grid size, it also shows the accuracy of the code.

Table 3: Dimensionless B. L. Thickness and its Percent Error

Grid Size	Dimensionless b.l. (true)	Dimensionless b.l. (program)	Percent % for b.l. Thickness
30 x 30	5	5.17	3.4
40 x 40	5	5.13	2.6
50 x 50	5	5.10	2
60 x 60	5	5.08	1.6
70 x 70	***5***	***5.07***	***1.4***

6.2 Results for the Flat Plate Problem

For the normal flat plate problem, here are graphs that display the code's accuracy in comparison with the problem that was solved in Reference 5. In Figure 5a, u/u_∞ is shown on the x-axis**.** It ranges from 0 to 1.0. The y-axis is the normalized y known as y_{bar}. It ranges from 0 to about 25.0. The other variable of importance outside of the ones mentioned in Table I is Reynolds number, with a value of 1000. This graph is for a constant wall, implying that the temperature on the wall is constant, and for an adiabatic wall, which means there is no heat transfer. The shapes of the graphs resemble the normal u curve that falls within the boundary layer. In Figure 5b, the distance across the plate, x, is shown on the x-axis, ranging from 0 to 1. The y-axis represents the variation of the skin friction coefficient, C_f that ranges from 0.02 to 0.17. The shapes of the graph are hyperbolic and the true and experimental curves are similar in respect to their mathematical behavior. However, the percent error is around 31.7% in the constant wall case, while in the adiabatic case, the error is around 32%.

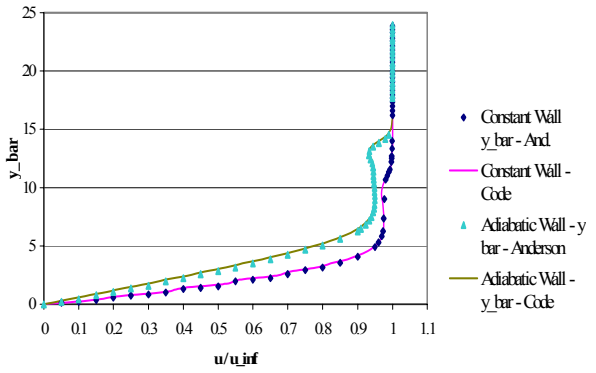

Figure 5a. Velocity component u vs. normalized y for constant temperature wall conditions and adiabatic wall conditions at the trailing edge

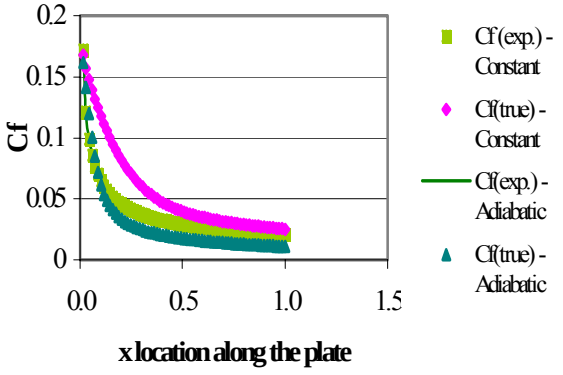

Figure 5b. Skin friction coefficient vs. x location along the plate for constant wall and adiabatic wall conditions

6.3 Results for the Hypersonic Boundary Layer/Shockwave Interaction Problem

For the hypersonic boundary layer/shockwave interaction problem, here are some of the contour plots that display the code's accuracy in comparison with the picture that was shown in Figure 3. The greatest accuracy shown takes place in the adiabatic wall condition plots. In these four figures, the x distance varies from 0.0 to 1.0 and the y distance varies from 0.0 to 0.3. Figure 6a depicts a contour plot with the highest distribution of v occurs just before the boundary layer/shockwave interaction and once that occurs, v slows down while at the section of the plate above the shockwave v stays constant. Within this plot and that in Figure 6b, there are little lines, which show the vector movement of the velocity components u and v within the plate. Once the lines hit the shock, their direction changes. Figure 6b represents a contour plot of v distribution for adiabatic wall conditions in the x-y domain and this particular contour plot resembles Figure 3, which displays boundary layer/shockwave interaction. The only difference between Figures 6b and 4 is that the flow requires a longer convergence time to form the reattachment shock. Figure 7a depicts a contour plot displaying as the shockwave appears, the value of temperature increases and the highest concentration of temperature occur slightly after the shockwave/boundary layer interaction forms. This occurs in a small area. Figure 7b depicts a contour plot of the value of temperature increases. The highest concentration occurs in close proximity of the plate. After the shockwave/boundary layer interaction takes place, the concentration of the temperature increases.

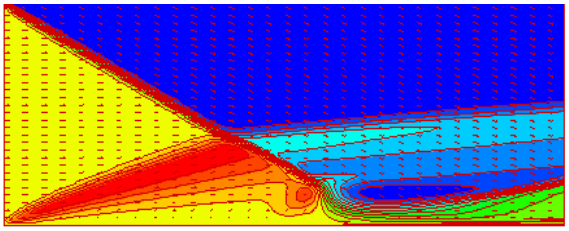

Figure 6a. Velocity component v distribution for constant temperature wall conditions

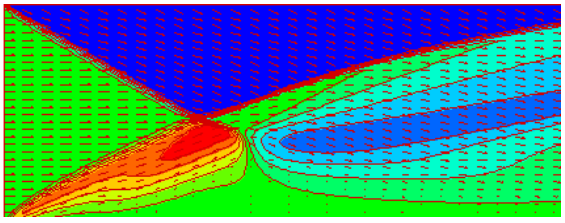

Figure 6b. Velocity component v distribution for adiabatic wall conditions

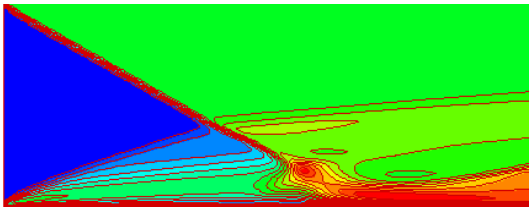

Figure 7a. Temperature distribution for constant temperature wall conditions

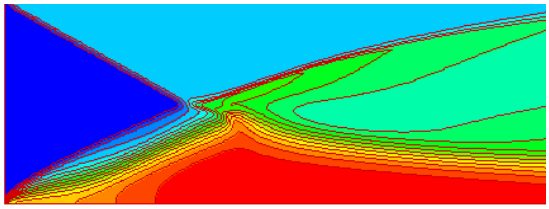

Figure 7b. Temperature distribution for adiabatic wall conditions

7.0 Conclusion

In this paper, a FORTRAN code was developed to solve the Navier-Stokes equations and prescribe boundary conditions using the MacCormack Corrector - Predictor Technique. The code was validated, by comparing results from the code with published texts. The results showed that this code is capable of solving the normal flat plate problem with prescribed freestream conditions and the boundary layer/shockwave interaction problem. Contour plots were developed in TECPLOT to display the behavior of the primitive variables u, v, temperature, and density on the plate. During each study, the results generated and the actions of the flow fields seem to be consistent.

8.0 Acknowledgements

This work has been partially sponsored by the following agencies; the National Institute of Aerospace, NASA Glenn and Langley Research Centers. In addition, special appreciation is extended to the Space Vehicle Technology Institute, one of the NASA University Institutes, with joint sponsorship from the Department of Defense. Appreciation is expressed to Claudia Meyer, Mark Klemm, Isaiah Blankson and Harry Cikanek of the NASA Glenn Research Center, and to Dr. John Schmisseur and Dr. Walter Jones of the Air Force Office of Scientific Research.

References

1. Schlichting, Herrmann. *Boundary Layer Theory.* Springer, 1999.

2. Grumet, Adam A. *A Numerical Study of Shockwave/Boundary Layer Interaction For Non Equilibrium Chemically Reacting Air: The Effects of Catalytic Walls*. University of Maryland College Park, 1990.

3. Ballaro, Charles A. *Shock Strength Effects On Separated Flows in Non-Equilibrium Chemically Reacting Air-Shockwave/Boundary Layer Interaction*. University of Maryland College Park, 1990.

4. Ozisik, M. Necati. *Finite Differencing Methods in Heat Transfer.* CRC Press, 1994.

5. Anderson, John. *Computational Fluid Dynamics.* McGraw Hill, 1995.

6. Kaviany, Massoud. *Principles of Heat Transfer.* Wiley Interscience, 2002.

7. Taylor, Thomas. *Computational Methods for Fluid Flow*. Springer-Verlag, 1983.

8. Abbot, M.B. *Computational Fluid Dynamics: An Introduction for Engineers.* Longman Scientific & Technical, 1989.

9. Mills, A.E. *Basic Heat & Mass Transfer.* Prentice Hall, 1999.

10. Anderson, Dale. *Computational Fluid Mechanics and Heat Transfer.* Hemisphere Publishing Corporation, 1984.

11. Anderson, John D. *Fundamentals of Aerodynamics.* McGraw-Hill, 1991.

12. Carafoli, Elie. *High-Speed Aerodynamics.* Pergamon Press, 1956.

13. Lindsay, Haile. *Hypersonic Boundary Layer/Shockwave Interaction.* North Carolina A&T State University, 2003.